

Communication: Probing the entrance channels of the $X + \text{CH}_4 \rightarrow \text{HX} + \text{CH}_3$ ($X = \text{F, Cl, Br, I}$) reactions via photodetachment of $X^- - \text{CH}_4$

Min Cheng,^{1,a)} Yuan Feng,^{1,a)} Yikui Du,¹ Qihe Zhu,¹ Weijun Zheng,^{1,b)} Gábor Czako,^{2,b)} and Joel M. Bowman²

¹National Laboratory of Molecular Sciences, State Key Laboratory of Molecular Reaction Dynamics, Institute of Chemistry, Chinese Academy of Sciences, Beijing 100190, China

²Cherry L. Emerson Center for Scientific Computation and Department of Chemistry, Emory University, Atlanta, Georgia 30322, USA

(Received 9 March 2011; accepted 25 April 2011; published online 20 May 2011)

The entrance channel potentials of the prototypical polyatomic reaction family $X + \text{CH}_4 \rightarrow \text{HX} + \text{CH}_3$ ($X = \text{F, Cl, Br, I}$) are investigated using anion photoelectron spectroscopy and high-level *ab initio* electronic structure computations. The pre-reactive van der Waals (vdW) wells of these reactions are probed for $X = \text{Cl, Br, I}$ by photodetachment spectra of the corresponding $X^- - \text{CH}_4$ anion complex. For $\text{F}^- - \text{CH}_4$, a spin-orbit splitting ($\sim 1310 \text{ cm}^{-1}$) much larger than that of the F atom (404 cm^{-1}) was observed, in good agreement with theory. This showed that in the case of the $\text{F}^- - \text{CH}_4$ system the vertical transition from the anion ground state to the neutral potentials accesses a region between the vdW valley and transition state of the early-barrier $\text{F} + \text{CH}_4$ reaction. The doublet splittings observed in the other halogen complexes are close to the isolated atomic spin-orbit splittings, also in agreement with theory. © 2011 American Institute of Physics. [doi:10.1063/1.3591179]

Photodetachment spectroscopy of a stable anion to produce a neutral reactive system has been proven to be a powerful probe of key properties of the reactive potential energy surface, such as the pre-reactive van der Waals (vdW) well and/or the reaction transition state (TS).¹⁻⁷ The sensitivity of this technique to probe these aspects of the reactive potential depends on the position of the anion vibrational wave function with respect to the vdW well and/or TS.

Examples where the power of this spectroscopy has been demonstrated include $\text{F} + \text{H}_2$,^{3,4} $\text{Cl} + \text{H}_2/\text{D}_2$,⁷ $X + \text{HX}'$ ($X, X' = \text{F, Cl, Br, I}$).⁸⁻¹¹ The extension to the $X + \text{CH}_4$ reactions, where X is a halogen, is currently underway in the laboratory of Neumark^{12,13} for F and Cl and also by us. This work complements the beautiful crossed molecular beam studies of the $\text{F} + \text{CH}_4$ and $\text{Cl} + \text{CH}_4$ reactions.¹⁴⁻¹⁹ Furthermore, our work presents the first characterization of the seemingly similar Br and I + CH_4 reactions.

In this communication we report a joint experimental and theoretical study of the low-resolution photodetachment spectra of the anions $X^- - \text{CH}_4$ ($X = \text{F, Cl, Br, I}$) and determine the regions probed on the neutral reactive potentials.

The $X^- - \text{CH}_4$ anions are stable complexes with single H-bonded equilibrium structures. Following the early work of Novoa *et al.*,²⁰ who reported the first computed interaction energies for $X^- - \text{CH}_4$ ($X = \text{F, Cl, Br, I}$), Bieske and co-workers studied the infrared spectra of $X^- - \text{CH}_4$.²¹⁻²⁴ Recently, two of us (G.C. and J.M.B.) reported highly accurate *ab initio* structure, dissociation energy, and vibrational spectrum for the $\text{F}^- - \text{CH}_4$ anion²⁵ as well as the accurate *ab initio* charac-

terization of the saddle point of the $\text{F} + \text{CH}_4$ reaction.²⁶ The $\text{F} + \text{CH}_4$ reaction has an early saddle point,^{26,27} whose structure slightly overlaps with that of the $\text{F}^- - \text{CH}_4$ anion; thus, it seems to be possible to probe the TS region of $\text{F} + \text{CH}_4$ by the photodetachment of $\text{F}^- - \text{CH}_4$ as shown in Fig. 1 and discussed in detail later. For $\text{Cl} - \text{CH}_4$ system, previous work showed that the anion equilibrium geometry overlaps with that of the vdW complex in the reactant valley,^{23,24,28} which was confirmed by the slow electron velocity-map imaging (SEVI) spectrum of $\text{Cl}^- - \text{CH}_4$ reported by Neumark.¹²

The experiments were conducted on a home-built set-up consisting of a time-of-flight (TOF) mass spectrometer and a magnetic-bottle photoelectron spectrometer, which has been described elsewhere.²⁹ Briefly, the $X^- - \text{CH}_4$ ($X = \text{F, Cl, Br, I}$) cluster anions were produced in a laser vaporization source by ablating a rotating, translating KX ($X = \text{F, Cl, Br, I}$, respectively) target with the second harmonic (532 nm) laser of a Nd:YAG laser, while the CH_4 gas with 5 atm. backing pressure was allowed to expand through a pulsed valve over the target. The formed cluster anions were mass analyzed by a TOF mass spectrometer. The cluster anions of interest were mass selected by a mass gate and then decelerated before photodetachment by the fourth harmonic (266 nm) of a second Nd:YAG laser. The flight time of the photoelectrons was measured by the magnetic-bottle photoelectron spectrometer. The electron binding energies (EBE) were obtained as usual by $\text{EBE} = h\nu - \text{EKE}$, where $h\nu$ is the photon energy, and EKE is the kinetic energy of the photoelectron. The photoelectron spectra were calibrated with known spectra of F^- , Cl^- , Br^- , and I^- .

The photoelectron spectra of X^- and $X^- - \text{CH}_4$ ($X = \text{F, Cl, Br, I}$) taken with 266 nm photons are shown in Fig. 2 and the observed spectra data are listed in Table I. The

^{a)} Also at Graduate University of Chinese Academy of Sciences.

^{b)} Authors to whom correspondence should be addressed. Electronic mail: zhengwj@iccas.ac.cn (W.Z.) and czako@chem.elte.hu (G.C.).

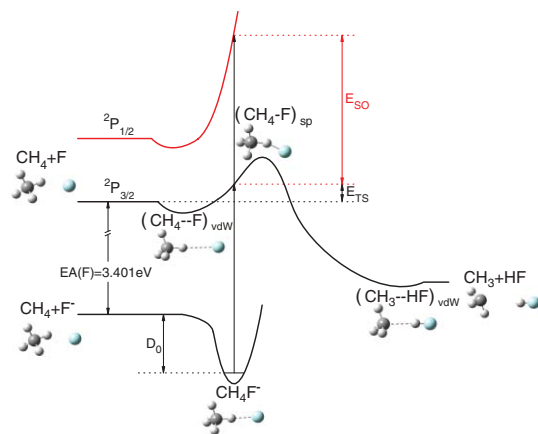


FIG. 1. Diagram of the potentials of the F^-CH_4 and $F-CH_4$ systems.

vertical detachment energy (VDE) shifts of X^-CH_4 relative to the VDEs of the corresponding X^- are shown in Fig. 3. The anions were produced in supersonic beams; thus, they stay at their vibrational ground state. Therefore, each peak in the spectra corresponds to a transition from the ground vibrational state of the anions to the ground or excited electronic states of the corresponding neutral system. The doublet features of the spectra show the energy difference between two electronic states of the neutral system. The error bar of the experimental results is determined to be ± 0.020 eV (± 0.010 eV for the splittings); thus, we cannot resolve the vibrational features corresponding to large amplitude motions (hindered rotations and intermolecular stretchings) of the neutral system. Note that Neumark and co-workers have probed F^-CH_4 ¹³ and Cl^-CH_4 ¹² by SEVI and found interesting spectral peaks whose assignment is still “a work in progress.”

In order to understand the doublet spectral peaks, the equilibrium structures of the anions as well as the loca-

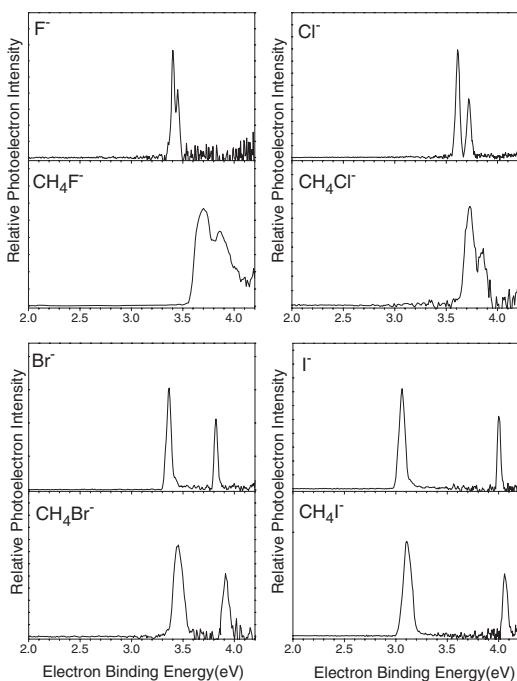


FIG. 2. Photoelectron spectra of X^- and X^-CH_4 ($X = F, Cl, Br, I$) taken with 266 nm photons.

TABLE I. Vertical detachment energies and their spin-orbit splittings (all in eV) for X^- and X^-CH_4 ($X = F, Cl, Br, I$).

	X^-		X^-CH_4			
	VDE	SO splitting	VDE	SO splitting		
F^-	$^2P_{3/2}$	3.401 ^a	F^-CH_4	$^2P_{3/2}$	3.701	0.163
	$^2P_{1/2}$	3.451	$^2P_{1/2}$	$^2P_{1/2}$	3.864	
Cl^-	$^2P_{3/2}$	3.613 ^a	Cl^-CH_4	$^2P_{3/2}$	3.730	0.124
	$^2P_{1/2}$	3.722	$^2P_{1/2}$	$^2P_{1/2}$	3.854	
Br^-	$^2P_{3/2}$	3.364 ^a	Br^-CH_4	$^2P_{3/2}$	3.447	0.465
	$^2P_{1/2}$	3.821	$^2P_{1/2}$	$^2P_{1/2}$	3.912	
I^-	$^2P_{3/2}$	3.059 ^a	I^-CH_4	$^2P_{3/2}$	3.108	0.949
	$^2P_{1/2}$	4.002	$^2P_{1/2}$	$^2P_{1/2}$	4.057	

^aReferences 37, 38, 39, and 40 for F, Cl, Br, and I, respectively.

tions of the TS (saddle point (SP) on the potential) and vdW wells of the neutrals have to be determined. Therefore, we have performed electronic structure computations by MOLPRO (Ref. 30) using high-level *ab initio* methods, i.e., [CCSD(T)]³¹ and [MRCI+Q],^{32,33} with the aug-cc-pVNZ [$N = 2(D), 3(T), 4(Q)$] correlation consistent basis set family of Dunning and co-workers.^{34,35} The MRCI+Q computations provided the entrance channel potentials for the A_1 and E (assuming C_{3v} symmetry) non-relativistic electronic states as well as the three doubly degenerate spin-orbit (SO) states (e.g., see Fig. 4), which are involved in the dynamics of the $X + CH_4$ reactions. The computed structures and energetics of the stationary points of the X^-CH_4 and $X-CH_4$ potentials are presented in Table II. The SO states and the SO splittings as a function of the C–X distance of the neutral systems are shown in Fig. S1 in the supplementary material (SM).³⁶ Further computational details are given in the footnote of Table II as well as in the SM.³⁶

The $F + CH_4$ reaction has an early saddle point ($F-H_b-CH_3$)_{SP}, whose structure slightly overlaps with that of F^-CH_4 , though the anion has longer H_b-F distance (1.844 Å) than the saddle point value (1.628 Å). Furthermore, ($F-H_b-CH_3$)_{SP} has C_s symmetry with $\angle F-H_b-C \approx 150^\circ$, whereas the point-group symmetry of F^-CH_4 is C_{3v} . (The energy difference between the C_s and C_{3v} ($F-H_b-CH_3$)_{SP} is, however,

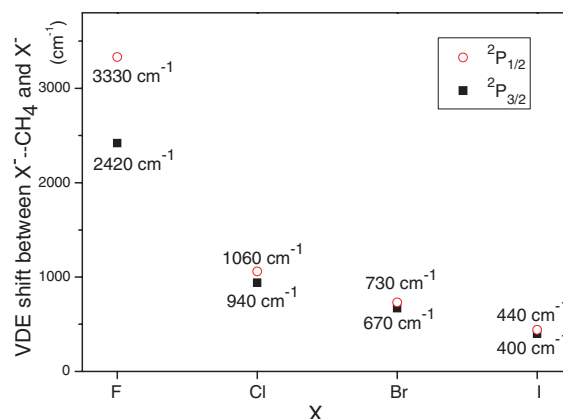


FIG. 3. VDE shifts of X^-CH_4 relative to the VDEs of the corresponding X^- . The difference in these “doublet numbers” is the difference between the doublet splittings of X^-CH_4 and X^- in Fig. 2.

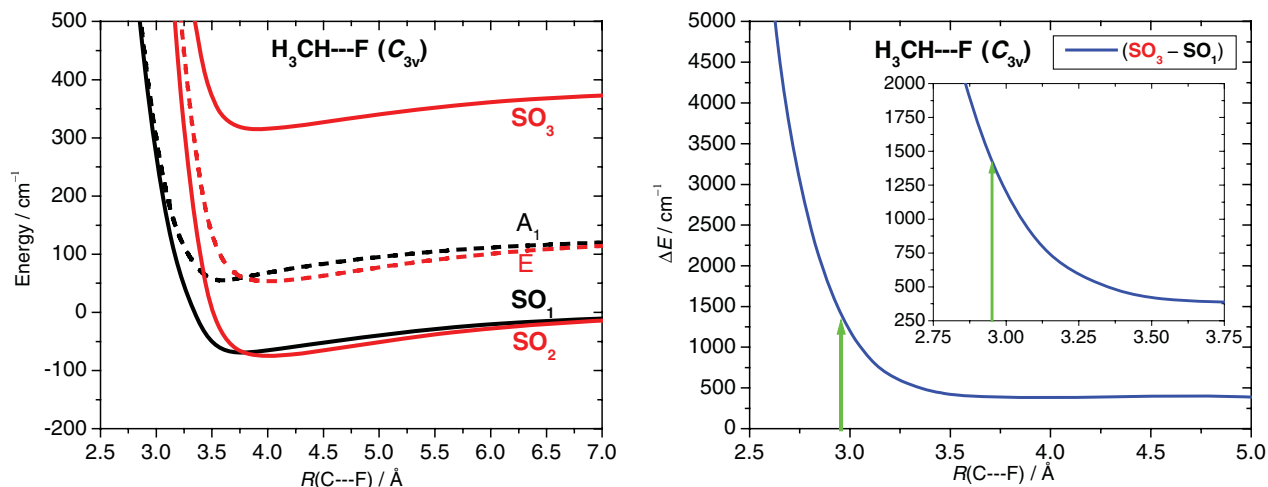


FIG. 4. Potential energy curves (left panel) and spin-orbit splittings (right panel) of $\text{CH}_4\text{-F}$ as a function of the C-F distance along the C_{3v} axis with fixed $\text{CH}_4(\text{eq})$ geometry and C-H-F linear bond arrangement computed at the MRCl+Q/aug-cc-pVTZ level of theory. A_1 and E denote the ground and excited non-SO states, respectively. SO_1 , SO_2 , and SO_3 are the three doubly degenerate SO states. The green arrows indicate the C-F equilibrium distance in the anion complex and the corresponding vertical splitting of the neutral system.

only a few cm^{-1} .) The $\text{H}_b\text{-F}$ distance at the shallow vdW minima ($\text{F-H}_b\text{-CH}_3$)_{vdW} is about 2.6–2.8 Å; thus, the structure of $\text{F}^-\text{-CH}_4$ corresponds to a configuration between the vdW and SP regions of the $\text{F} + \text{CH}_4$ reaction. Indeed the VDE shift between $\text{F}^-\text{-CH}_4$ and $\text{F}(^2P_{3/2})$ (2420 cm^{-1}) is larger than the D_0 value of $\text{F}^-\text{-CH}_4$ (2337 cm^{-1}); thus, the experiment probes the neutral potential above the reactant asymptote by about 100 cm^{-1} , which is less than the SO-corrected barrier height ($\sim 270 \text{ cm}^{-1}$) as expected considering the above mentioned structural parameters.

Computations show that the $X + \text{CH}_4$ ($X = \text{Cl}, \text{Br},$ and I) reactions have late barriers, with increasing classical heights of 2711, 6402, and 10574 cm^{-1} , respectively, and the corresponding saddle-point structures do not overlap with

those of the anions (see Table II). The CH_4 geometries in the anion complexes are almost free CH_4 equilibrium structures [$r(\text{CH}) = 1.088 \text{ \AA}$], whereas the CH_b distances of $(X\text{-H}_b\text{-CH}_3)_{\text{SP}}$ are 1.407, 1.687, and 1.972 Å for Cl, Br, and I, respectively. Therefore, in these cases the anion photodetachment measurements probe the vdW regions of the neutral reactions. Indeed, the anion structures overlap with the corresponding $(X\text{-H}_b\text{-CH}_3)_{\text{vdW}}$ structure, though the $X\text{-H}_b$ distances are slightly shorter in the anions in all the cases of $X = \text{Cl}, \text{Br},$ and I . The measured VDE shifts between $X\text{-CH}_4(^2P_{3/2})$ and $X(^2P_{3/2})$ are 940, 670, 400 cm^{-1} , whereas the computed D_0 values of $X^-\text{-CH}_4$ are 971, 788, 605 cm^{-1} for $X = \text{Cl}, \text{Br},$ and I , respectively (see Table II). These results indicate that the experiments access the vdW wells for Cl, Br,

TABLE II. Computed structures (in Å and degrees) and relative energies (dissociation energies and barrier heights in cm^{-1}) of the $X^-\text{-CH}_4$ anion complexes as well as the entrance-channel vdW complexes and the saddle points of the $X + \text{CH}_4$ reactions ($X = \text{F}, \text{Cl}, \text{Br}, \text{I}$).

	State	$r(\text{C-H})^a$	$r(\text{C-H}_b)^a$	$r(\text{X-H}_b)^a$	$\alpha(\text{H-C-H}_b)^a$	$\Delta E_c [\Delta E_0]^{a,b}$
$(\text{F-H}_b\text{-CH}_3)^-$	1A_1	1.094	1.110	1.844	110.4	2475[2337]
$(\text{F-H}_b\text{-CH}_3)_{\text{vdW}}$	SO_1, SO_2, SO_3	1.088	1.088	2.6, 2.8, 2.7	109.5	79, 94, 85
$(\text{F-H}_b\text{-CH}_3)_{\text{SP}}$	$^2A_1'$	1.090/1.088 ^c	1.112 ^c	1.628 ^c	107.3/108.3 ^c	139[144]
$(\text{Cl-H}_b\text{-CH}_3)^-$	1A_1	1.091	1.093	2.639	109.8	1111[971]
$(\text{Cl-H}_b\text{-CH}_3)_{\text{vdW}}$	SO_1, SO_2, SO_3	1.088	1.088	3.0, 3.2, 3.1	109.5	116, 136, 123
$(\text{Cl-H}_b\text{-CH}_3)_{\text{SP}}$	2A_1	1.084	1.407	1.443	101.0	2711[1240]
$(\text{Br-H}_b\text{-CH}_3)^-$	1A_1	1.091	1.092	2.865	109.8	910[788]
$(\text{Br-H}_b\text{-CH}_3)_{\text{vdW}}$	SO_1, SO_2, SO_3	1.088	1.088	3.2, 3.3, 3.3	109.5	114, 131, 121
$(\text{Br-H}_b\text{-CH}_3)_{\text{SP}}$	2A_1	1.082	1.687	1.491	97.4	6402[4933]
$(\text{I-H}_b\text{-CH}_3)^-$	1A_1	1.090	1.090	3.188	109.7	708[605]
$(\text{I-H}_b\text{-CH}_3)_{\text{vdW}}$	SO_1, SO_2, SO_3	1.088	1.088	3.4, 3.5, 3.5	109.5	130, 148, 137
$(\text{I-H}_b\text{-CH}_3)_{\text{SP}}$	2A_1	1.095 ^d	1.972 ^d	1.658 ^d	94.9 ^d	10574[8919] ^d

^a*Ab initio* results obtained at the CCSD(T)/aug-cc-pVQZ and ROHF-UCCSD(T)/aug-cc-pVTZ levels of theory for the anions and the saddle points, respectively. For the vdW complexes CCSD(T)/aug-cc-pVQZ $\text{CH}_4(\text{eq})$ structures and MRCl+Q/aug-cc-pVTZ $X\text{-H}_b$ distances are given. For Br and I small-core pseudopotentials and the corresponding basis sets were employed. All the complexes have C_{3v} symmetry, except $(\text{F-H}_b\text{-CH}_3)_{\text{SP}}$ (C_s).

^b $\Delta E_c [\Delta E_0]$ denotes the $D_c [D_0]$ values for the anion and vdW complexes and classical [ground state vibrationally adiabatic] barrier heights for the saddle points. The harmonic zero-point energy corrections were computed at CCSD(T)/aug-cc-pVTZ. For the vdW complexes the D_c values were obtained at MRCl+Q/aug-cc-pVTZ for the spin-orbit (SO_1, SO_2, SO_3) states (see Fig. 4).

^c $(\text{F-H}_b\text{-CH}_3)_{\text{SP}}$ has C_s point-group symmetry and $\alpha(\text{C-H}_b\text{-F}) = 152^\circ$ (see more details in Ref. 26).

^dThese values were computed at the ROHF-UCCSD(T)/aug-cc-pVDZ level of theory.

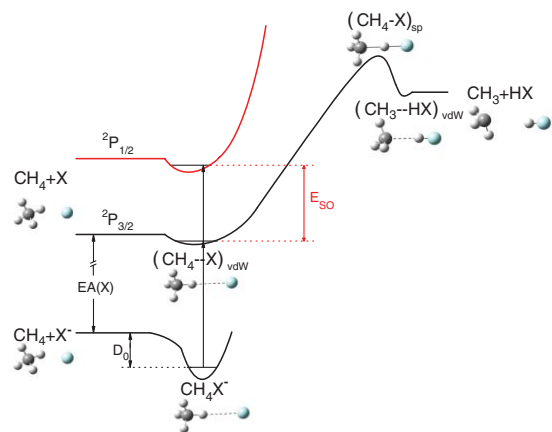


FIG. 5. Diagram of the potentials of the X^-CH_4 and $X-CH_4$ systems ($X = Cl, Br, I$).

and I, since the VDE shifts are smaller than the D_0 values of the corresponding anion complexes.

The SO splittings in the photodetachment spectra of X^-CH_4 and X^- provide very useful information about the regions where the neutral potentials are probed. The most interesting case is the $X = F$, where the measured SO splitting between $F(^2P_{3/2})$ and $F(^2P_{1/2})$ is 0.050 eV (404 cm^{-1}) whereas the spectrum of F^-CH_4 is split by 0.163 eV (1310 cm^{-1}). The measured doublet splitting of the F^-CH_4 complex is larger than the SO splitting of F by ~ 0.113 eV, which is quite significant. Fig. 4 shows the computed SO splitting as a function of the C-F separation. As seen, the measured SO splitting of F^-CH_4 nicely corresponds to the computed splitting considering vertical transitions from the anion potential to the neutral SO surfaces. The SO splitting also reveals that we do not probe the vdW valley, since the splitting would be very close to the atomic limit in the vdW well. Furthermore, the computations predict an even much larger doublet splitting at the saddle point indicating that the photodetachment does not access the saddle point. The schematic of $F^-CH_4 \rightarrow F^-CH_4 + e^-$ is shown in Fig. 1, where, as indicated, the anion wave function is projected on to the neutral surface in a region between the vdW well and the reaction saddle point.

For $X = Cl, Br$, and I , the measured SO splittings of the X^-CH_4 complexes are larger than the splittings of X by only $\sim 0.015, 0.008$, and 0.006 eV, respectively, in good agreement with theory as shown in Fig. S1 of the SM.³⁶ These are much smaller than in the case of F^-CH_4 (~ 0.113 eV), showing that we probe the vdW regions of the $Cl, Br, I + CH_4$ reactions (see Fig. 5).

Overall, the combination of anion photoelectron spectroscopy experiment and *ab initio* electronic structure computations presents a clear picture of the entrance channel potentials of $X + CH_4 \rightarrow HX + CH_3$ ($X = F, Cl, Br, I$) reactions. The spin-orbit splitting information of the $F + CH_4$ reaction is confirmed for the first time. The nice agreement between the experiment and theory indicates that the theoretical methods used here can also be extended to other similar reactions.

G.C. thanks the NSF (CRIF:CRF CHE-0625237) and J.M.B. also thanks the DOE (DE-FG02-97ER14782) for financial support. W.Z. acknowledges the Institute of Chemistry, Chinese Academy of Sciences for start-up funds.

- ¹D. M. Neumark, *Annu. Rev. Phys. Chem.* **43**, 153 (1992).
- ²D. M. Neumark, *Acc. Chem. Res.* **26**, 33 (1993).
- ³D. E. Manolopoulos, K. Stark, H. J. Werner, D. W. Arnold, S. E. Bradforth, and D. M. Neumark, *Science* **262**, 1852 (1993).
- ⁴A. Weaver and D. M. Neumark, *Faraday Discuss. Chem. Soc.* **91**, 5 (1991).
- ⁵D. M. Neumark, *Science* **272**, 1446 (1996).
- ⁶P. G. Wenthold, D. A. Hrovat, W. T. Borden, and W. C. Lineberger, *Science* **272**, 1456 (1996).
- ⁷E. Garand, J. Zhou, D. E. Manolopoulos, M. H. Alexander, and D. M. Neumark, *Science* **319**, 72 (2008).
- ⁸A. Weaver, R. B. Metz, S. E. Bradforth, and D. M. Neumark, *J. Phys. Chem.* **92**, 5558 (1988).
- ⁹R. B. Metz, T. Kitsopoulos, A. Weaver, and D. M. Neumark, *J. Chem. Phys.* **88**, 1463 (1988).
- ¹⁰R. B. Metz, A. Weaver, S. E. Bradforth, T. N. Kitsopoulos, and D. M. Neumark, *J. Phys. Chem.* **94**, 1377 (1990).
- ¹¹R. B. Metz, and D. M. Neumark, *J. Chem. Phys.* **97**, 962 (1992).
- ¹²D. M. Neumark, *J. Phys. Chem. A* **112**, 13287 (2008).
- ¹³D. M. Neumark, personal communications, 2007 and 2011.
- ¹⁴J. J. Lin, J. G. Zhou, W. C. Shiu, and K. P. Liu, *Science* **300**, 966 (2003).
- ¹⁵W. Q. Zhang, H. Kawamata, and K. P. Liu, *Science* **325**, 303 (2009).
- ¹⁶W. Shiu, J. J. Lin, and K. P. Liu, *Phys. Rev. Lett.* **92**, 103201 (2004).
- ¹⁷B. Zhang and K. Liu, *J. Chem. Phys.* **122**, 101102 (2005).
- ¹⁸G. Czako, Q. Shuai, K. Liu, and J. M. Bowman, *J. Chem. Phys.* **133**, 131101 (2010).
- ¹⁹F. Wang, J.-S. Lin, and K. Liu, *Science* **331**, 900 (2011).
- ²⁰J. J. Novoa, M. H. Whangbo, and J. M. Williams, *Chem. Phys. Lett.* **180**, 241 (1991).
- ²¹D. A. Wild, Z. M. Loh, and E. J. Bieske, *Int. J. Mass. Spectrom.* **220**, 273 (2002).
- ²²Z. M. Loh, R. L. Wilson, D. A. Wild, E. J. Bieske, J. M. Lisy, B. Njagic, and M. S. Gordon, *J. Phys. Chem. A* **110**, 13736 (2006).
- ²³D. A. Wild, Z. M. Loh, P. P. Wolyneec, P. S. Weiser, and E. J. Bieske, *Chem. Phys. Lett.* **332**, 531 (2000).
- ²⁴Z. M. Loh, R. L. Wilson, D. A. Wild, E. J. Bieske, and M. S. Gordon, *Aust. J. Chem.* **57**, 1157 (2004).
- ²⁵G. Czako, B. J. Braams, and J. M. Bowman, *J. Phys. Chem. A* **112**, 7466 (2008).
- ²⁶G. Czako, B. C. Shepler, B. J. Braams, and J. M. Bowman, *J. Chem. Phys.* **130**, 084301 (2009).
- ²⁷G. Czako and J. M. Bowman, *J. Am. Chem. Soc.* **131**, 17534 (2009).
- ²⁸K. Hiraoka, T. Mizuno, T. Iino, D. Eguchi, and S. Yamabe, *J. Phys. Chem. A* **105**, 4887 (2001).
- ²⁹H.-G. Xu, Z.-G. Zhang, Y. Feng, J. Y. Yuan, Y. C. Zhao, and W. J. Zheng, *Chem. Phys. Lett.* **487**, 204 (2010).
- ³⁰MOLPRO, a package of *ab initio* programs designed by H.-J. Werner and P. J. Knowles, version 2008.1, R. D. Amos, A. Bernhardsson, A. Berning *et al.*, see <http://www.molpro.net>.
- ³¹K. Raghavachari, G. W. Trucks, J. A. Pople, and M. Head-Gordon, *Chem. Phys. Lett.* **157**, 479 (1989).
- ³²H.-J. Werner and P. J. Knowles, *J. Chem. Phys.* **89**, 5803 (1988).
- ³³P. J. Knowles and H.-J. Werner, *Chem. Phys. Lett.* **145**, 514 (1988).
- ³⁴T. H. Dunning, *J. Chem. Phys.* **90**, 1007 (1989).
- ³⁵R. A. Kendall, T. H. Dunning, and R. J. Harrison, *J. Chem. Phys.* **96**, 6796 (1992).
- ³⁶See supplementary material at <http://dx.doi.org/10.1063/1.3591179> for further computational details.
- ³⁷C. Blondel, C. Delsart, and F. Goldfarb, *J. Phys. B* **34**, L281 (2001).
- ³⁸U. Berzins, M. Gustafsson, D. Hanstorp, A. E. Klinkmueller, U. Ljungblad, and A.-M. Martensson-Pendrill, *Phys. Rev. A* **51**, 231 (1995).
- ³⁹C. Blondel, P. Cacciani, C. Delsart, and R. Trainham, *Phys. Rev. A* **40**, 3698 (1989).
- ⁴⁰D. Hanstorp and M. Gustafsson, *J. Phys. B* **25**, 1773 (1992).